Airborne EM Imaging for Coastal Aquifer Management in Muravera, Sardinia, Italy

J. Moilanen [1], M.C. Porru [2], Y. Podmogov [3], C. Arras [2], E. Karshakov [1], G. Vignoli [2], S. Da Pelo [2], A. Moilanen [3]

[1] V.A. Trapeznikov Institute of Control Sciences of Russian Academy of Sciences; [2] University of Cagliari; [3] Geotechnologies

Summary

An EQUATOR helicopter-borne AEM survey (~1,500 line-km, 200 m spacing) over the Muravera coastal plain (Flumendosa delta, SE Sardinia) produced a quasi-3D resistivity volume that refines hydrostratigraphy and informs groundwater management. The AEM model maps discontinuous shallow conductive horizons (1–10 Ω·m) interpreted as lagoonal silts/clays or brackish deposits, moderately resistive phreatic alluvium (10–50 Ω·m), and more resistive gravelly/coarse alluvial axes (≈30–150 Ω·m). Crucially, it delineates a laterally extensive deep conductive lagoonal clay unit (≈0.5–5 Ω·m) acting as an aquitard, previously inferred only from sparse boreholes. Resistivity patterns support a pathway-controlled salinization model, with discontinuous conductive bodies and preferential-flow corridors (paleochannels, river mouths, foxi, abstraction-driven upconing) rather than a uniform seawater wedge.

For management, AEM results

(1) delineate salinity-prone domains,

(2) identify transmissive coarse bodies that can propagate drawdown and salinity, and

(3) indicate areas where small head changes yield large salinity responses.

The survey prioritizes locations for targeted follow-up (TEM, ERT/IP, borehole logging, hydrochemistry, head-EC monitoring) and recommends calibrated, uncertainty-aware integration with borehole and petrophysical data to support vulnerability zoning, monitoring design, and abstraction scenarios.

Airborne EM Imaging for Coastal Aquifer Management in Muravera, Sardinia, Italy

Introduction

Coastal aquifers are difficult management targets because groundwater quality is controlled by the coupled effects of recharge variability, abstraction, surface-water regulation, geological heterogeneity and seawater intrusion. The Muravera alluvial plain in southeastern Sardinia, Italy, is an emblematic case. It extends along the terminal reach of the Flumendosa River and opens toward the Tyrrhenian Sea. The plain includes coastal lagoons, abandoned river branches locally known as foxi, engineered river mouths and a seasonal irrigation weir, all of which modify hydraulic gradients and river-aquifer exchange during the irrigation season.

Previous hydrogeological, hydrochemical, isotopic and ground-geophysical investigations have shown that the system is not a simple homogeneous coastal aquifer (Porru, 2023). It includes a shallow phreatic aquifer, a deeper partially confined alluvial aquifer, low-permeability lagoonal and clay-rich units, and a salinity distribution that varies both laterally and vertically. However, the key limitation for management has been the spatial extrapolation of point-scale evidence. Stratigraphic logs, electrical-conductivity profiles and ground-based geophysical lines provide strong constraints locally, but they cannot, alone, define the basin-scale continuity of conductive lagoonal bodies, coarse alluvial axes, paleovalley geometries and possible saline pathways.

Here, we briefly present the acquisition, preliminary processing and geological interpretation of helicopter-borne airborne electromagnetic (AEM) data collected over the Muravera plain in 2023 (Fig. 1). The objective is not only to map resistivity, but to translate the AEM-derived resistivity volume into a defensible hydrogeological interpretation that can support vulnerability zoning, monitoring design and scenario analysis for groundwater abstraction in a coastal aquifer affected by salinization.

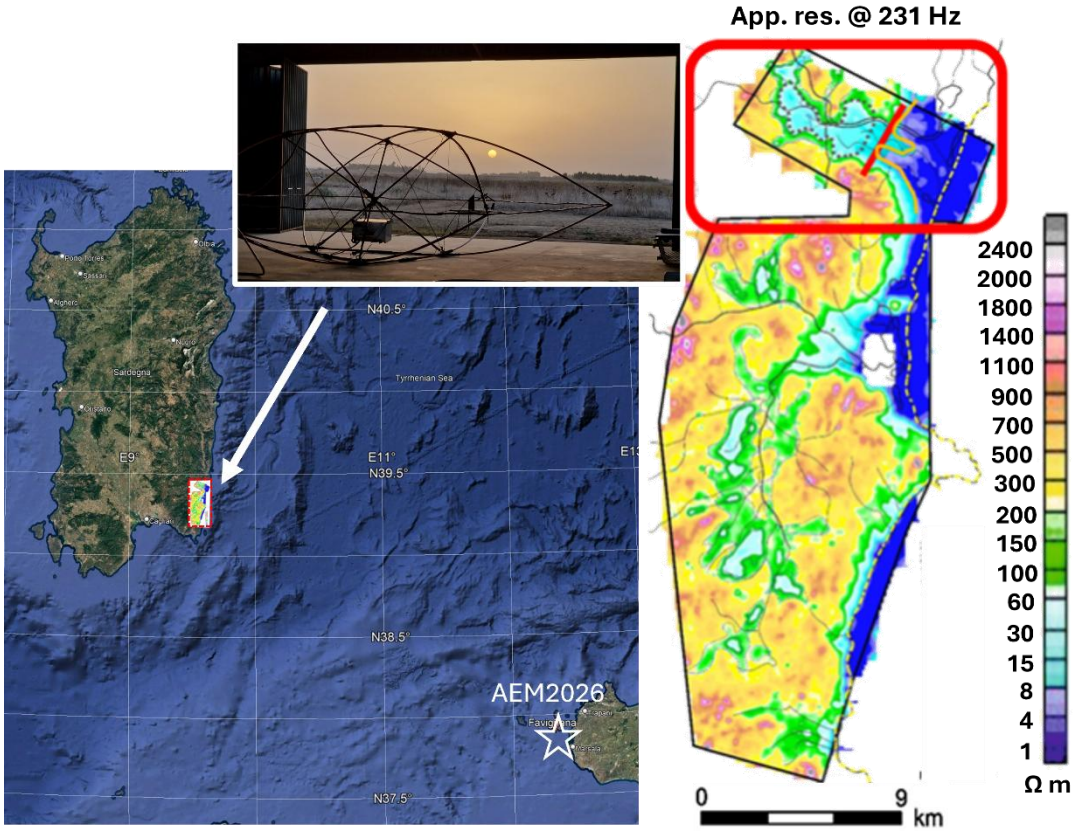


Figure 1 *Location of the survey (with respect to the AEM2026 venue); Image of the EQUATOR system; Map of the measured apparent resistivity at 231 Hz.*

AEM acquisition and inversion

The AEM survey collected approximately 1500 line-km of co-located electromagnetic and magnetic data over the Flumendosa coastal plain and adjacent sectors. The nominal line spacing was about 200 m, allowing the generation of a quasi-3D resistivity model at a scale appropriate for hydrostratigraphic interpretation. The data were acquired with the EQUATOR towed helicopter system (Karshakov et al., 2017), which records full-time time-domain responses at 200 kHz sampling, with a 6.6 Hz output rate, a base frequency of 77 Hz and a dipole moment up to about 100,000 Am². The operational survey speed was of the order of 100 km/h, while the compact towed configuration allowed acquisition in a coastal plain characterized by infrastructure, power lines, agricultural areas and local topographic constraints.

The processing workflow was designed to preserve as much usable data as possible while reducing non-geological noise. Particular attention was paid to anthropic electromagnetic interference, which can affect specific frequencies and propagate into the time-domain response, especially at late times. After data conditioning, the AEM responses were inverted using a layered 1D forward approximation to obtain a quasi-3D electrical resistivity volume (Karshakov, 2020). Concerning the interpretation, even from these preliminary results was clear the adherence of the retrieved resistivity ranges and spatial structures with the geological conceptual model (Fig. 2) of the area based on preexisting knowledge and measurements.

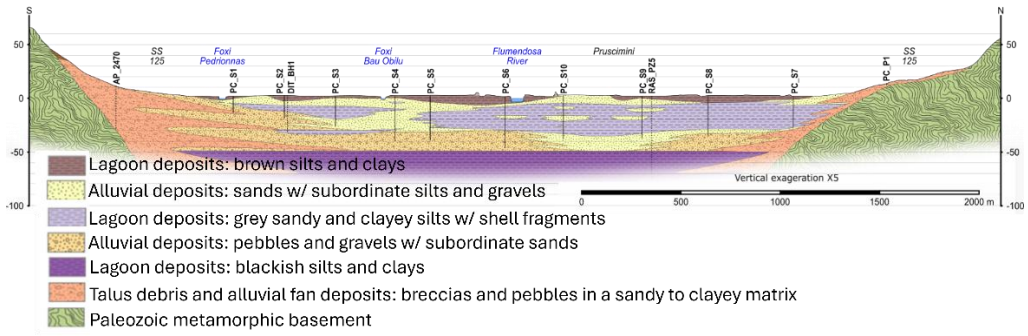


Figure 2 *Conceptual model (after Porru, 2023).*

The working interpretation follows two principles. First, in coastal aquifers, low resistivity may reflect saline or brackish pore water, clay-rich sediments, or both; conversely, higher resistivity may indicate coarser freshwater-saturated alluvium, alluvial-fan deposits or basement. Second, because 1D AEM inversion can be biased by lateral resistivity gradients and 3D effects, the deterministic section shown below should be considered a geologically constrained interpretation, not a unique solution. Future refinement should include petrophysical calibration and explicit treatment of forward-modelling and interpretation uncertainty (Bai et al., 2021; Zaru et al., 2024).

Results and geological interpretation

The AEM-derived resistivity patterns confirm that the Muravera coastal aquifer is strongly heterogeneous and compartmentalized. The vertical section selected for Figure 3 crosses the sector where the resistivity model is most informative for hydrogeological interpretation. Shallow conductive horizons, generally in the order of 1-10 Ωm, are interpreted as lagoonal silts and clays and locally as brackish shallow deposits. These units are discontinuous, but where present they can cap permeable alluvial deposits and contribute to semi-confined or perched hydraulic conditions.

Below and laterally adjacent to these shallow conductors, moderately resistive domains, commonly around 10-50 Ωm, are compatible with the phreatic alluvial aquifer made of sands with subordinate silts and gravels. Their resistivity is expected to vary markedly with pore-water salinity. More resistive packages, typically about 30-150 Ωm but locally lower where brackish, are interpreted as semi-confined gravelly to pebbly alluvial bodies and coarse alluvial axes. These bodies are hydrogeologically relevant because they may act as preferential flow or stress-propagation corridors during seasonal abstraction.

The most important new result is the basin-scale definition of the deeper conductive body, locally around 0.5-5 Ωm, interpreted as a laterally extensive lagoonal clayey unit acting as a low-permeability aquiclude or aquitard. Before the airborne survey, the existence of brackish lagoonal silts and clays was supported mainly by sparse boreholes and local measurements; their lateral continuity, thickness and internal variability remained uncertain. The AEM volume transforms this unit from an extrapolated hypothesis into a mapped hydrostratigraphic element that can be included explicitly in vulnerability zoning and scenario analysis.

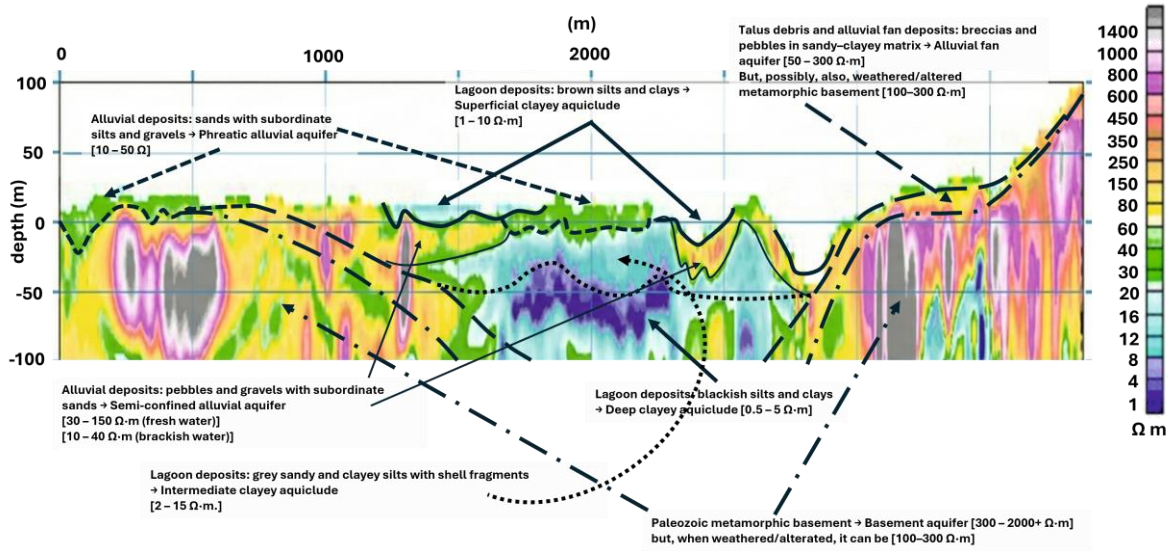


Figure 3 *One vertical section extracted from the quasi-3D AEM resistivity volume, with the current geological interpretation.*

The resistivity distribution also argues against a purely two-dimensional, laterally continuous seawater wedge. Conductive anomalies occur as discontinuous bodies embedded within more resistive alluvial material. This supports a pathway-controlled conceptual model, in which salinization may occur through hydraulically connected corridors, paleochannel or lagoonal bodies, river-mouth and foxi-related connections, and local abstraction-induced upconing. At the margins of the plain, higher resistivity values, commonly 50-300 Ωm and locally higher than 300 Ωm, are consistent with alluvial-fan deposits and the Paleozoic metamorphic basement. Nevertheless, overlap between weathered basement, coarse fan deposits and freshwater-saturated alluvium remains possible in intermediate resistivity ranges, reinforcing the need for multi-evidence interpretation

Implications for groundwater management

From a management perspective, the AEM data refine aquifer vulnerability in three ways. First, they delineate salinity-prone domains associated with conductive coastal-lagoonal units and deep conductive pathways that could not be mapped reliably from point observations alone. Second, they identify resistive coarse alluvial bodies that may transmit drawdown and salinity perturbations efficiently, especially during irrigation-season abstraction. Third, they indicate where small head variations may cause disproportionate salinity responses, particularly in sectors where permeable bodies are hydraulically connected to conductive lagoonal or coastal units.

The AEM model therefore provides a spatial framework for deciding where local follow-up information has the highest value. Targeted ground TEM, ERT/IP, borehole logging, hydrochemical sampling and continuous head-EC monitoring can be focused where the resistivity model indicates high ambiguity or high vulnerability. This iterative workflow is particularly important for the Muravera plain because the seasonal irrigation weir, managed river releases, coastal lagoons and abandoned river branches produce transient boundary conditions. During summer, saline water can move inland along the lower Flumendosa and related coastal-water bodies, and withdrawals may enhance river-to-aquifer exchange

or local upconing. AEM does not replace hydrological monitoring, but it provides the spatial architecture needed to interpret those time series in a process-based way.

The main interpretational limitation is non-uniqueness. Bulk resistivity integrates lithology, porosity, saturation and pore-water conductivity; hence, a conductive anomaly cannot automatically be assigned to clay or saline groundwater without geological and hydrochemical control. For this reason, the Muravera interpretation deliberately retains uncertainty and emphasizes hydrostratigraphic plausibility rather than a single deterministic facies map. The next step should be a calibrated, uncertainty-aware integration of the AEM volume with borehole data, water electrical conductivity, petrophysical constraints and 3D geological modelling (Zaru et al., 2023).

Conclusions

The Muravera AEM survey demonstrates the value of dense airborne electromagnetic mapping for coastal aquifers where salinization is controlled by the combined effects of geology, surface-water regulation and abstraction. The 2023 EQUATOR survey provides a quasi-3D resistivity volume that spatially constrains lagoonal clay-rich units, alluvial aquifer bodies, potential paleovalley or preferential-flow structures and the geometry of salinity-prone domains. The key advance relative to previous point-based and profile-based information is the explicit basin-scale mapping of a conductive lagoonal package that strongly influences vulnerability but was previously poorly constrained.

The resulting interpretation supports a conceptual model in which seawater intrusion and brackish-water occurrence are not represented by a single uniform wedge, but by discontinuous and pathway-controlled conductive domains. This has direct implications for monitoring-network design, abstraction assessment and risk-based zoning. The Muravera case therefore illustrates how AEM can move from reconnaissance geophysics to decision-support hydrogeology, provided that resistivity models are interpreted jointly with geological, hydrochemical and hydraulic evidence and that non-uniqueness is treated as a decision-relevant quantity.

Acknowledgements (Optional)

The airborne geophysical survey and related interpretation were developed within the PNRR MUR RETURN project, "Multi-Risk Science for Resilient Communities under a Changing Climate" (PE00000005), and in cooperation between the University of Cagliari, the Sardinian Hydrographic District Agency and ARPAS. The authors acknowledge the availability of previous hydrogeological and hydrochemical datasets.

References

Bai, P., Vignoli, G. and Hansen, T.M. [2021]. 1D stochastic inversion of airborne time-domain electromagnetic data with realistic prior and accounting for the forward modeling error. Remote Sensing, 13(19), 3881.

Karshakov, E.V. [2020]. Iterated extended Kalman filter for airborne electromagnetic data inversion. Exploration Geophysics, 51(1), 66-73.

Karshakov, E.V., Podmogov, Y.G., Kertsman, V.M. and Moilanen, J. [2017]. Combined frequency domain and time domain airborne data for environmental and engineering challenges. Journal of Environmental and Engineering Geophysics, 22(1), 1-11.

Porru, M.C. [2023]. Caratterizzazione idrogeologica avanzata dell'acquifero alluvionale della piana costiera di Muravera. PhD thesis, University of Cagliari.

Zaru, N., Rossi, M., Vacca, G. and Vignoli, G. [2023]. Spreading of localized information across an entire 3D electrical resistivity volume via constrained EMI inversion based on a realistic prior distribution. Remote Sensing, 15(16), p.3993.

Zaru, N., Silvestri, S., Assiri, M., Bai, P., Hansen, T.M. and Vignoli, G. [2024]. Probabilistic petrophysical reconstruction of Danta's Alpine peatland via electromagnetic induction data. Earth and Space Science, 11(3), p.e2023EA003457.